Bioorganic & Medicinal Chemistry Letters 25 (2015) 668–672

Contents lists available at ScienceDirect

Bioorganic & Medicinal Chemistry Letters

journal homepage: www.elsevier.com/locate/bmcl

Structure-based design, synthesis and biological evaluation of novel β-secretase inhibitors containing a pyrazole or thiazole moiety as the P3 ligand

Arun K. Ghosh [a,b,c,*], Margherita Brindisi [a,b], Yu-Chen Yen [d], Xiaoming Xu [a,b], Xiangping Huang [a,e], Thippeswamy Devasamudram [c,f], Geoffrey Bilcer [c,f], Hui Lei [f], Gerald Koelsch [a,e,f], Andrew D. Mesecar [a,d], Jordan Tang [a,e,g]

[a] Department of Chemistry, Purdue University, West Lafayette, IN 47907, United States
[b] Department of Medicinal Chemistry, Purdue University, West Lafayette, IN 47907, United States
[c] Department of Chemistry, University of Illinois at Chicago, Chicago, IL 60607, United States
[d] Department of Biological Sciences, Purdue University, West Lafayette, IN 47907, United States
[e] Protein Studies Program, Oklahoma Medical Research Foundation, United States
[f] CoMentis Inc, Oklahoma City, OK 73104, United States
[g] Department of Biochemistry and Molecular Biology, University of Oklahoma Health Science Center, Oklahoma City, OK 73104, United States

ARTICLE INFO

Article history:
Received 21 October 2014
Revised 26 November 2014
Accepted 28 November 2014
Available online 6 December 2014

Keywords:
β-secretase
Alzheimer's disease
Memapsin 2
BACE-1
Protease inhibitors

ABSTRACT

We describe structure-based design, synthesis, and biological evaluation of a series of novel inhibitors bearing a pyrazole (compounds **3a**–**h**) or a thiazole moiety (compounds **4a**–**e**) as the P3 ligand. We have also explored Boc-β-amino-L-alanine as a novel P2 ligand. A number of inhibitors have displayed β-secretase inhibitory potency. Inhibitor **4c** has shown potent BACE1 inhibitory activity, K_i = 0.25 nM, cellular EC_{50} of 194 nM, and displayed good selectivity over BACE2. A model of **4c** was created based upon the X-ray structure of **2**-bound β-secretase which revealed critical interactions in the active site.

The development of effective treatment for Alzheimer's disease (AD) continues to be a formidable challenge in medicine.[1,2] β-Secretase (also known as memapsin 2 or BACE1) is the protease responsible for the first cleavage of β-amyloid precursor protein (APP) leading to the production of a 40/42 residue amyloid-β-peptides (Aβ), the major constituent of the brain amyloid plaques.[3,4] The pathological hallmark of AD is the formation of amyloid plaques and neurofibrillary tangles in the brain of AD patients, which is generally believed to be derived from Aβ accumulation and intimately related to the pathogenesis of AD. Due to the central role of β-secretase in the generation of Aβ, inhibition of β-secretase has become a major focus in the search for AD therapy.[5–7] From a therapeutic perspective, BACE1 inhibition has generated much interest as a suitable target since BACE1 gene deletion in mice showed only a mild phenotypic response.[8,9] Despite the promise of BACE1 as a target, the clinical development of a BACE1 inhibitor has been quite slow and challenging.[10] This is due to problems associated with poor pharmacological properties of inhibitors, particularly the inability to cross the blood–brain-barrier and the lack of inhibitor selectivity against other important human aspartic acid proteases.[11–13]

Early reports from our laboratories demonstrated that a potent BACE1 inhibitor can be designed by incorporating a nonhydrolyzable Leu-Ala hydroxyethylene dipeptide isostere at the cleavage site.[14,15] As shown, inhibitor **1** (OM99-2, Fig. 1) is quite potent. We subsequently determined the X-ray crystal structure of **1**-bound BACE1 which provided insight into ligand-binding site interactions and critical drug design templates.[7] Inhibitor **1** did not show selectivity over BACE2 or cathepsin D (Cat-D). We then reported the design of potent and selective inhibitors. Peptidomimetic inhibitor **2** with a pyrazolemethyl urethane showed excellent potency and selectivity over BACE2 (>3800-fold) and Cat-D (>2500-fold).[16] Based upon the X-ray crystal structure of **2**-bound β-secretase, we further explored amide-based P2–P3 ligands. Herein we report our studies in which we have developed pyrazole and thiazole-derived novel P3-ligands containing hydrogen bond

* Corresponding author.

http://dx.doi.org/10.1016/j.bmcl.2014.11.087
0960-894X/

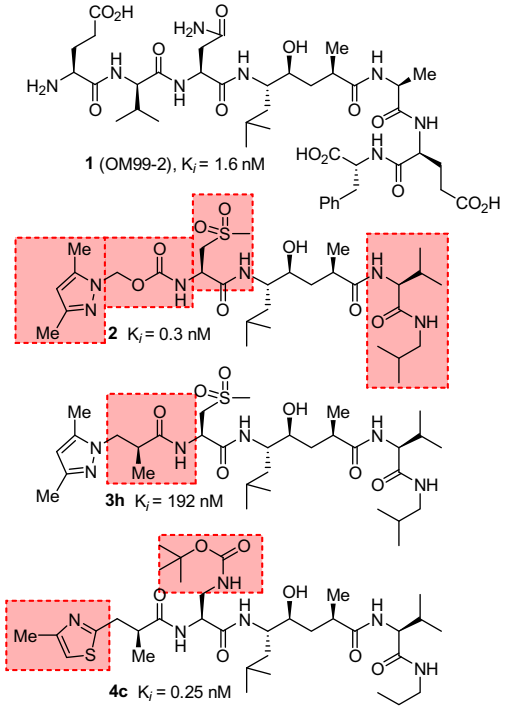

Figure 1. Structures of BACE1 inhibitors **1**, **2**, **3h** and **4c**.

donor and acceptor groups to interact with residues in the S3 subsite. Asymmetric synthesis of these heterocyclic ligands as well as the use of optically active (1*S*,2*R*)-1-tosyl-amino-2-indanol provided access to optically pure ligands.

The synthesis of the pyrazole-derived ligands is shown in Scheme 1. Reaction of 3,5-dimethyl pyrazole **5** and methyl methacrylate in a sealed tube at 180 °C for 6 h provided racemic Michael addition product **6**.[17] Saponification of ester **6** with aqueous LiOH at 23 °C for 10 h furnished the corresponding racemic acid. Esterification of the acid with (1*S*,2*R*)-1-tosyl-amino-2-indanol[18,19] using EDC and DMAP at 23 °C for 12 h afforded a diastereomeric mixture (nearly 1:1 by ^{1}H NMR analysis) of esters, **7a** and **7b**. The mixture was separated by silica gel chromatography to provide pure diastereomers, **7a** and **7b**. The absolute configuration of the α-methyl center of diastereomer **7a** was determined by X-ray crystallographic analysis. Saponification of esters **7a** and **7b** using aqueous LiOH at 23 °C for 10 h furnished optically active ligand acids (*S*)-**8** and (*R*)-**8**.

For the synthesis of optically active ligands containing other substitutions, dimethylmalonate **9** was converted to acrylate derivatives **10a–c** as described in the literature.[20] These acrylate derivatives were converted to pyrazole derivatives **11a–c** by Michael addition in the presence of 3,5-dimethyl pyrazole **5** as described above. Saponification and subsequent esterification with (1*S*,2*R*)-1-tosyl-amino-2-indanol afforded the diastereomeric mixture of esters. Diastereomers were separated by silica gel chromatography and the respective diastereomer with the lower R_f-value turned out to be the isomer with the (*S*)-configuration at the α-alkyl center. Further corroboration of stereochemistry of the α-alkyl group was carried out by comparison of ^{1}H NMR data with diastereomer **7a**. Saponification of esters provided optically active ligand acids (*S*)-**12a–c**. Acid (*S*)-**14**, containing a 3-methylpyrazole moiety, was prepared following the same procedures described for (*S*)-**8**.

The synthesis of the thiazole acids is shown in Scheme 2. For asymmetric alkylation, (*R*)-4-benzyl-2-oxazolidinone derivatives **15a**,**b** were prepared as described previously.[21] Treatment of

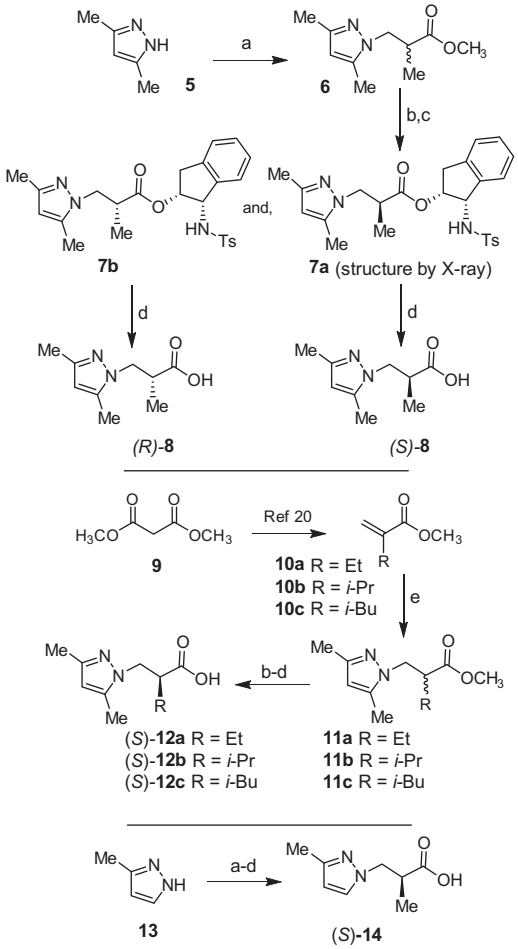

Scheme 1. Reagents and conditions: (a) methyl methacrylate, 6 h, 180 °C, sealed tube, 59–61%; (b) LiOH·H_2O, H_2O/THF, 23 °C, 10 h, 73–80%; (c) (1*S*,2*R*)-(−)-*cis*-1-tosyl-amino-2-indanol, EDC, DMAP, dry CH_2Cl_2, 23 °C, 12 h, 62–90%; (d) LiOH·H_2O, H_2O/THF, 23 °C, 10 h, 54–60%: (e) 3,5-dimethyl-1*H*-pyrazole, 6 h, 180 °C, sealed tube, 59–62%.

oxazolidinone **15a** with NaHMDS in THF at −78 °C provided the corresponding enolate.[22] The enolate was reacted with known 4-iodomethyl-2-methylthiazole **16**[23] at −78 °C to 23 °C for 1 h furnishing alkylated product **17a** diastereoselectively. Alkylation of **15b** with iodide **16** provided alkylated product **17b**. Subsequent treatment of **17a**,**b** with a mixture of aqueous LiOH and hydrogen peroxide at 0 °C for 1 h afforded optically active ligand acids **18a** and **18b**, respectively.

For the synthesis of isomeric ligand acids, commercially available (4-methylthiazole-2-yl) methanol **19** was converted to 2-iodomethyl-4-methylthiazole **20** by treatment of **19** with mesyl chloride and triethylamine followed by reaction of the resulting mesylate with lithium iodide in acetone. Asymmetric alkylation of oxazolidinone derivatives **15a–c** with iodide **20** as described above afforded alkylation products **21a–c**, respectively. Removal of the chiral auxiliary with alkaline hydrogen peroxide furnished optically active ligand acids **22a–c**.

The synthesis of inhibitors is shown in Scheme 3. Commercially available protected β-amino-L-alanine **23** was coupled with Leu-Ala transition-state isostere derivative **24** in the presence of EDC, HOBt and diisopropylethylamine at 23 °C for 15 h to provide amide derivative **25** in good yield. Removal of the Cbz-group by catalytic hydrogenation over Pearlman's catalyst furnished amine **26** in near quantitative yield. Coupling of this amine with ligand acid (*S*)-**8** followed by removal of the TBS group by exposure to TBAF in

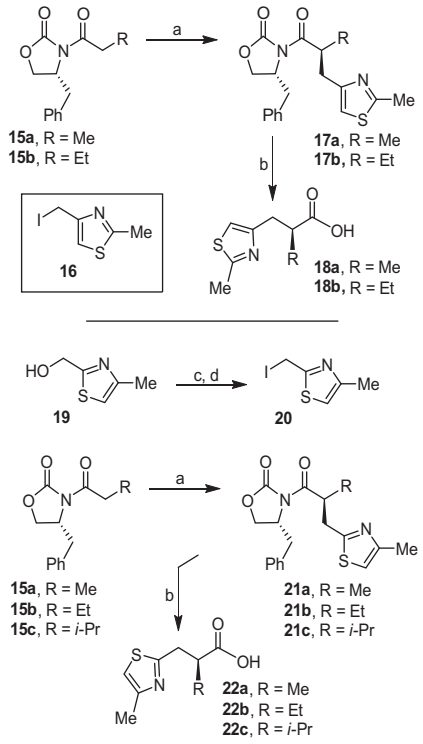

Scheme 2. Reagents and conditions: (a) NaHMDS (1 M in THF), **16** or **20**, dry THF, −78 °C to 23 °C, 1 h, 69–86%; (b) LiOH·H_2O, 30% wt H_2O_2, H_2O/THF, 0 °C, 1 h, 90–95%; (c) CH_3SO_2Cl, TEA, dry CH_2Cl_2, 1 h, 0 °C; (d) LiI, acetone, 2 h, 23 °C, 82% (over two steps).

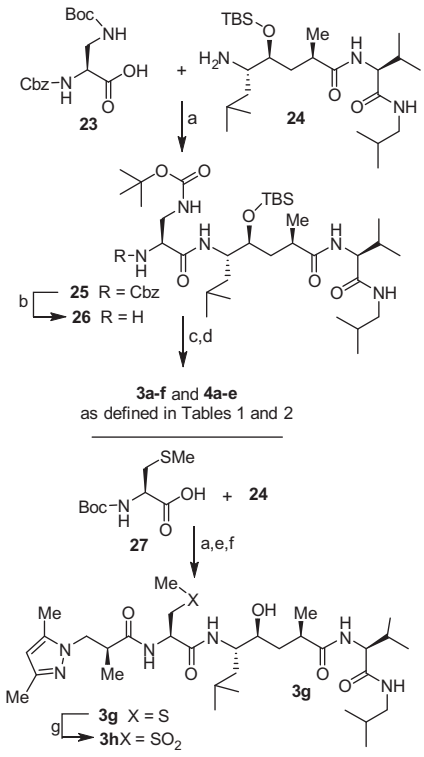

Scheme 3. Reagents and conditions: (a) EDCI·HCl, HOBt·H_2O, DIPEA, dry CH_2Cl_2, dry DMF, 23 °C, 15 h, 61%; (b) $Pd(OH)_2$ 20% on carbon, H_2, MeOH, 3 h, 99%; (c) appropriate carboxylic acid, EDCI·HCl, HOBt·H_2O, DIPEA, DMF, 15 h, 23 °C, 45–52%; (d) TBAF, THF, 23 °C, 12 h, 65–72%; (e) TFA, CH_2Cl_2, 2 h, 23 °C, 98%; (f) (*S*)-**8**, HATU, HOAt, 2,4,6-collidine, DMF, 23 °C, 15 h, 68%; (g) Oxone, MeOH, water, 23 °C, 1.5 h, 99%.

THF provided inhibitor **3a**. Inhibitors **3b–f** were synthesized by following a similar sequence of reactions as inhibitor **3a**.

For the synthesis of inhibitors **3g**,**h**, amine **24** was coupled with commercially available *N*-Boc-L-methylcysteine **27** using EDC and HOBt to furnish the corresponding coupled product. Removal of the Boc group by exposure to trifluoroacetic acid, followed by coupling of the resulting amine with optically active ligand acid (*S*)-**8** directly provided inhibitor **3g** without needing the final TBS deprotection step. Oxidation of the sulfide with oxone furnished inhibitor **3h** in excellent yield.[24] The synthesis of inhibitors **4a–e** was carried out by coupling amine **26** with thiazole-derived ligand acids **18a**,**b** and **22a–c** to furnish the corresponding coupling products. Exposure of the coupling products to TBAF in THF as described for inhibitor **3a**, afforded inhibitors **4a–e**.

The β-secretase inhibitory activity was determined against recombinant β-secretase using our previously reported assay protocols.[25] The structure and inhibitory potency of inhibitors **3a–h** and **4a–e** are reported in Tables 1 and 2, respectively. As can be observed, the activity data generated from the pyrazole-containing inhibitors (Table 1) clearly outline a series of well-defined structure-activity relationships (SARs). First of all, the (*S*)-configuration of the α-alkyl group showed to be of critical importance for the inhibitory activity, as demonstrated by the dramatic drop in potency (nearly 40-fold) for compound **3b** with respect to **3a**, bearing the α-methyl group with (*R*)-configuration. This series of compounds also highlighted the efficacy of the small alkyl group at the α-position, as shown by the steady loss in inhibitory potency with the increase of the steric bulk of the α-alkyl group (**3a** > **3c** > **3e** > **3d**). Compound **3d**, bearing the bulkier α-isopropyl group displayed a nearly 10-fold reduction of potency compared to inhibitor **3a**. The importance of both methyl groups on the pyrazole ring (**3a**) can be seen by comparison of its inhibitory activity with that of inhibitor **3f**. This evidence is in line with the molecular insight obtained from the protein–ligand X-ray structure of the pyrazole-bearing inhibitor **2**.[16] In this X-ray structure, both methyl groups on the pyrazole ring appear to effectively fill the S3 hydrophobic pocket. The importance of Boc-β-amino-L-alanine as the P2 ligand over methylsulfonyl-L-alanine can be seen by comparison of inhibitor **3a** with **3h**. Interestingly, methyl sulfide derivative **3g** turned out to be more potent in this series than methyl sulfone derivative **3h**.[17]

Thiazole containing compounds were also evaluated against β-secretase and their inhibitory potencies are reported in Table 2. Compound **4a** with a 2-methylthiazole moiety and α-methyl group in the P3 ligand showed good BACE1 activity. However, compound **4c**, bearing the 4-methylthiazole moiety in the P3 ligand turned out to be a very potent inhibitor with over 120-fold improvement over inhibitor **4a**. The corresponding inhibitors bearing an ethyl group or an isopropyl group (**4d** and **4e**) were significantly less active.

We have determined the cellular production of Aβ in BE(2)-M17 human neuroblastoma cells (ATCC® CRL-2267™).[26] Inhibitor **4c** displayed an EC_{50} value of 194 nM in this assay. It showed good selectivity against memapsin 1 (K_i = 71 nM, selectivity >280-fold). However, its selectivity over Cat-D was marginal (K_i = 1.25 nM, 5-fold). As mentioned, blood–brain barrier (BBB) penetration represents a major issue for the development of BACE1 inhibitors.[11–13] It appears that the lipophilicity of inhibitor **4c** (*c*log*P*, 3.55) is improved compared to urethane-derived inhibitor **2** (*c*log*P*, 2.21).[27,28] Such improvement of lipid solubility may favor BBB penetration of compound **4c** over compound **2**.

To obtain molecular insight into specific ligand-binding site interactions, we created an energy-minimized active site model of inhibitor **4c** based upon the crystal structure of inhibitor **2**-bound β-secretase.[16] The conformation of **4c** was optimized using the CHARMM force field.[29] A stereoview of the model is shown in

Table 1
Enzyme inhibitory activity of pyrazole-based inhibitors **3a–h**

Entry	Inhibitor	K_i (nM)
1	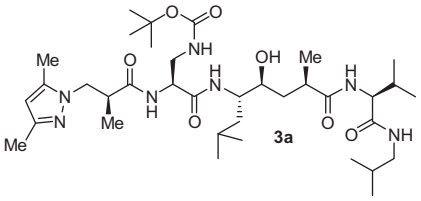 **3a**	40
2	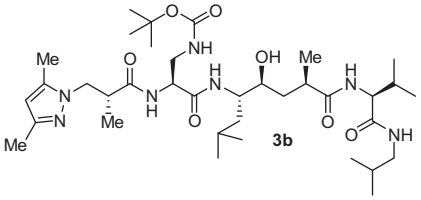 **3b**	1640
3	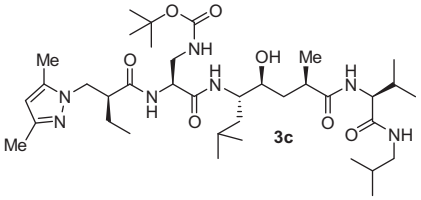 **3c**	63.1
4	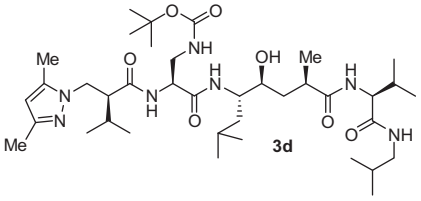 **3d**	471
5	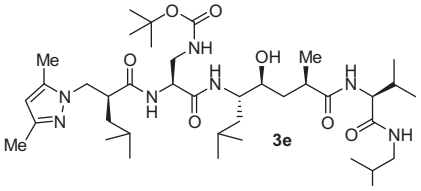 **3e**	147.7
6	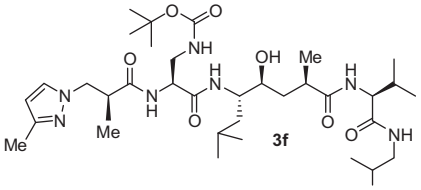 **3f**	201
7	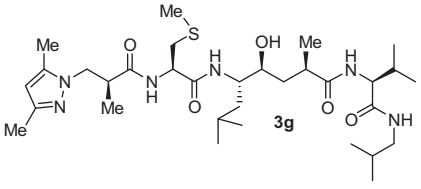 **3g**	64.2
8	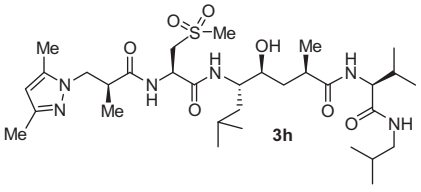 **3h**	192.2

Table 2
Enzyme inhibitory activity of thiazole containing inhibitors **4a–e**

Entry	Inhibitor	K_i (nM)
1	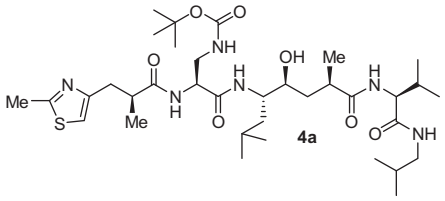 **4a**	31.9
2	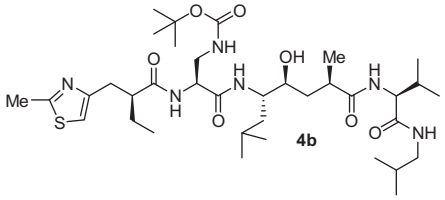 **4b**	16.8
3	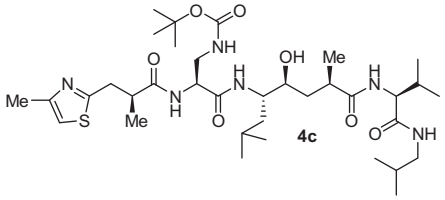 **4c**	0.25
4	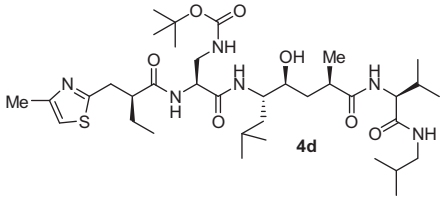 **4d**	10.8
5	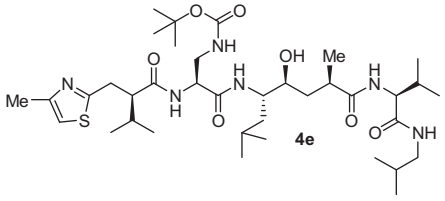 **4e**	28.9

Figure 2. As it appears, the P3-thiazole nitrogen is within proximity to form a hydrogen bond with the Thr232 side chain hydroxyl group. The P3-ligand carbonyl oxygen is also within hydrogen bonding distance to the Thr232 backbone NH. The methyl group on the thiazole ring seems to fill in the shallow hydrophobic pocket in the S3 subsite of BACE1. Similarly, the (*S*)-methyl group occupies a hydrophobic pocket surrounding Gly11, Ile110, Lys 107 and Gln73. Preference for the (*S*)-configuration can be justified as the alkyl group with (*R*)-configuration appears to bump into the P1-leucine side chain, which may likely destabilize ligand binding site interactions in the S3-pocket.

The P2 Boc-aminomethyl functionality appears to fit nicely in the S2-subsite. As shown, the Boc-carbonyl oxygen can form a hydrogen bond with the Gln73 side chain carboxamide. Also, the Boc-NH and the urethane oxygen are well positioned to make a water-mediated hydrogen bond with the backbone NH of Asn233 and the P3-ligand carbonyl oxygen. These interactions of the P2 and P3 ligands may be responsible for the observed selectivity of inhibitor **4c** over BACE2. The transition-state hydroxyl group of inhibitor **4c** forms a number of hydrogen bonds with the active site aspartic acid residues Asp32 and Asp228. These interactions and other inhibitor **4c**-BACE1 interactions in the S1′–S3′ subsites are similar to inhibitor **2**.[16]

In summary, we have carried out structure-based design and synthesis of novel P2–P3 ligands for BACE1 inhibitors containing Leu-Ala hydroxyethylene isosteres. In particular, we have designed pyrazole and thiazole-derived P3-ligands which contain hydrogen bond donor and acceptor groups for specific interactions in the S3 subsite. We have developed a practical asymmetric synthesis of

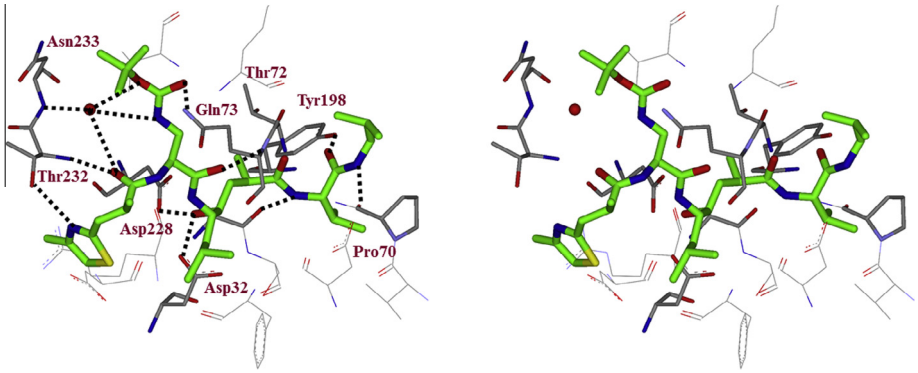

Figure 2. Stereoview of the model of inhibitor **4c** (green carbon chain) with β-secretase. Possible hydrogen bonds between the inhibitor and β-secretase are shown in black dotted lines.

these heterocyclic ligands using readily available optically active (1*S*,2*R*)-aminoindan-2-ol derivatives. We have also investigated Boc-amino alanine and methylsulfonyl alanine as the P2-ligands. The Boc-amino alanine ligand provided an inhibitor with enhanced activity compared to inhibitors with a P2-methylsulfonyl derivative. Inhibitor **4c** displayed excellent BACE1 inhibitory activity and good selectivity over BACE2. Its cellular inhibitory potency in neuroblastoma cells was in the micromolar range. An energy-minimized model of inhibitor **4c** was created based upon the X-ray structure of **2**-bound β-secretase. This model has provided important molecular insight into the ligand-binding site interactions in the S2 and S3 subsites of β-secretase. Further design and improvement of inhibitor properties are currently in progress.

Acknowledgments

Financial support by the National Institutes of Health and Purdue University is gratefully acknowledged. Partial support by the Walther Cancer Foundation (ADM) is also gratefully acknowledged. J.T. held the J.G. Peuterbaugh Chair at the Oklahoma Medical Research Foundation during the course of this work. We would also like to thank Dr. Kalapala Venkateswara Rao (Purdue University) and Ms. Heather Osswald (Purdue University) for helpful discussions.

References and notes

1. Ghosh, A. K.; Brindisi, M.; Tang, J. *J. Neurochem.* **2012**, *120*(Suppl 1), 71.
2. Ghosh, A. K.; Gemma, S.; Tang, J. *Neurotherapeutics* **2008**, *5*, 399.
3. Selkoe, D. J.; Schenk, D. *Annu. Rev. Pharmacol.* **2003**, *43*, 545.
4. Citron, M. *Trends Pharmacol. Sci.* **2004**, *25*, 92.
5. Vassar, R.; Kovacs, D. M.; Yan, R.; Wong, P. C. *J. Neurosci.* **2009**, *29*, 12787.
6. Evin, G.; Barakat, A.; Masters, C. L. *Int. J. Biochem. Cell Biol.* **2010**, *42*, 1923.
7. Hong, L.; Koelsch, G.; Lin, X.; Wu, S.; Terzyan, S.; Ghosh, A. K.; Zhang, X. C.; Tang, J. *Science* **2000**, *290*, 150.
8. Luo, Y.; Bolon, B.; Kahn, S.; Bennett, B. D.; Babu-Khan, S.; Denis, P.; Fan, W.; Kha, H.; Zhang, J.; Gong, Y.; Martin, L.; Louis, J. C.; Yan, Q.; Richards, W. G.; Citron, M.; Vassar, R. *Nat. Neurosci.* **2001**, *4*, 231.
9. Cai, H.; Wang, Y.; McCarthy, D.; Wen, H.; Borchelt, D. R.; Price, D. L.; Wong, P. C. *Nat. Neurosci.* **2001**, *4*, 233.
10. Ghosh, A. K.; Osswald, H. L. *Chem. Soc. Rev.* **2014**, *43*, 6765.
11. Roberds, S. L.; Anderson, J.; Basi, G.; Bienkowski, M. J.; Branstetter, D. G.; Chen, K. S.; Freedman, S. B.; Frigon, N. L.; Games, D.; Hu, K.; Johnson-Wood, K.; Kappenman, K. E.; Kawabe, T. T.; Kola, I.; Kuehn, R.; Lee, M.; Liu, W.; Motter, R.; Nichols, N. F.; Power, M.; Robertson, D. W.; Schenk, D.; Schoor, M.; Shopp, G. M.; Shuck, M. E.; Sinha, S.; Svensson, K. A.; Tatsuno, G.; Tintrup, H.; Wijsman, J.; Wright, S.; McConlogue, L. *Hum. Mol. Genet.* **2001**, *10*, 1317.
12. Fischer, F.; Molinari, M.; Bodendorf, U.; Paganetti, P. *J. Neurochem.* **2002**, *80*, 1079.
13. Benes, P.; Vetvicka, V.; Fusek, M. *Crit. Rev. Oncol. Hematol.* **2008**, *68*, 12.
14. Ghosh, A. K.; Bilcer, G.; Harwood, C.; Kawahama, R.; Shin, D.; Hussain, K. A.; Hong, L.; Loy, J. A.; Nguyen, C.; Koelsch, G.; Ermolieff, J.; Tang, J. *J. Med. Chem.* **2001**, *44*, 2865.
15. Ghosh, A. K.; Kumaragurubaran, N.; Hong, L.; Kulkarni, S. S.; Xu, X.; Chang, W.; Weerasena, V.; Turner, R.; Koelsch, G.; Bilcer, G.; Tang, J. *J. Med. Chem.* **2007**, *50*, 2399.
16. Ghosh, A. K.; Kumaragurubaran, N.; Hong, L.; Lei, H.; Hussain, K. A.; Liu, C. F.; Devasamudram, T.; Weerasena, V.; Turner, R.; Koelsch, G.; Bilcer, G.; Tang, J. *J. Am. Chem. Soc.* **2006**, *128*, 5310.
17. Faissner, R.; Huttner, G.; Kaifer, E.; Rutsch, P. *Eur. J. Inorg. Chem.* **2003**, 1681.
18. Ghosh, A. K.; Onishi, M. *J. Am. Chem. Soc.* **1996**, *118*, 2527.
19. Ghosh, A. K.; Fidanze, S. *Synthesis* **1998**, 937.
20. Miller, R. B.; Smith, B. F. *Synth. Commun.* **1973**, *3*, 359.
21. Evans, D. A.; Bartroli, J.; Shih, T. L. *J. Am. Chem. Soc.* **1981**, *103*, 2127.
22. Evans, D. A.; Ennis, M. D.; Mathre, D. J. *J. Am. Chem. Soc.* **1982**, *104*, 1737.
23. Kajigaeshi, S.; Kawano, Y.; Fujisaki, S.; Kanemasa, S. *Heterocycles* **1985**, *23*, 2989.
24. Mccarthy, J. R.; Matthews, D. P.; Paolini, J. P. *Org. Synth.* **1995**, *72*, 209.
25. Ermolieff, J.; Loy, J. A.; Koelsch, G.; Tang, J. *Biochemisty* **2000**, *39*, 12450.
26. Macias, M. P.; Gonzales, A. M.; Siniard, A. L.; Walker, A. W.; Corneveaux, J. J.; Huentelman, M. J.; Sabbagh, M. N.; Decourt, B. *J. Neurosci. Methods* **2014**, *223*, 114.
27. *c*Log*P* was calculated using QikProp, version 3.4, Schrödinger, LLC, New York, NY, 2011.
28. Suenderhauf, C.; Hammann, F.; Huwyler, J. *Molecules* **2012**, *17*, 10429.
29. Brooks, B. R.; Brooks, C. L., III; Mackerell, A. D.; Nilsson, L.; Petrella, R. J.; Roux, B.; Won, Y.; Archontis, G.; Bartels, C.; Boresch, S.; Caflisch, A.; Caves, L.; Cui, Q.; Dinner, A. R.; Feig, M.; Fischer, S.; Gao, J.; Hodoscek, M.; Im, W.; Kuczera, K.; Lazaridis, T.; Ma, J.; Ovchinnikov, V.; Paci, E.; Pastor, R. W.; Post, C. B.; Pu, J. Z.; Schaefer, M.; Tidor, B.; Venable, R. M.; Woodcock, H. L.; Wu, X.; Yang, W.; York, D. M.; Karplus, M. *J. Comp. Chem.* **2009**, *30*, 1545.